Inert Gas Thruster Technology

Harold R. Kaufman,* Raymond S. Robinson,† and Donald C. Trock‡
Colorado State University, Fort Collins, Colorado

Some recent advances in component technology for inert gas thrusters are described. The maximum electron emission of a hollow cathode with argon can be increased 60-70% by the use of an enclosed keeper configuration. Operation with argon, but without emissive oxide, has also been obtained. A 30-cm thruster operated with argon at moderate discharge voltages gave double-ion measurements consistent with a double-ion correlation developed previously using 15-cm thruster data. An attempt was made to reduce discharge losses by biasing anodes positive of the discharge plasma. The reason this attempt was unsuccessful is not yet clear. The performance of a single-grid ion-optics configuration was evaluated. The ion impingement on the single-grid accelerator was found to approach the value expected from the projected blockage when the sheath thickness next to the accelerator was 2-3 times the aperture diameter.

Introduction

A CONTINUED research program has been directed at both component and overall performance of inert gas thrusters.[1-5] Progress is reported herein for component research in cathodes, discharge chambers, and ion optics.

A maximum electron emission has been observed for a given combination of cathode configuration and inert gas flow. Preliminary tests have previously shown that higher maximum emissions can be reached at the same gas flow using an enclosed-keeper design. Reported herein are the results of an experimental study of different enclosed-keeper configurations, with the study directed at increasing the maximum emission.

The "conventional" hollow-cathode configuration has a tungsten tip welded to a tantalum tube, together with an oxide-impregnated insert. When projected to larger sizes, thermal stresses at the welded joint could easily cause reliability problems. Also, there have been various problems associated with the presence of the oxide that is provided to enhance electron emission. A research effort has, therefore, been directed toward new hollow-cathode concepts. Among the more promising concepts, described herein, is a carbon-cathode tip held in place with spring tension. No emissive oxide is used with the carbon tip design, and heat is provided by an internal glow discharge.

Doubly charged ions are responsible for most of the erosion within a discharge chamber. To provide design information for future large thrusters, double ion data were obtained with a 30-cm multipole thruster.

Another area of discharge chamber research concerned the possible reflection of ions at the discharge chamber boundary. If such reflection were possible, it could result in reduced discharge losses. To this end, an experiment was conducted with various anode biases.

The final research described herein is the study of single-grid ion optics. The usual two- or three-grid ion optics become increasingly limited in current capacity as specific impulse is lowered. Single-grid ion optics are limited by sputtering erosion to low ion energies, but avoid the ion-beam current limitations of multiple-grid ion optics. The operating characteristics of a single-grid ion-optics configuration were measured to facilitate evaluation of this ion-optics approach at, for electrostatic propulsion, relatively low specific impulses.

Presented as Paper 81-0721 at the AIAA/JSASS/DGLR 15th International Electric Propulsion Conference, Las Vegas, Nev., April 21-23, 1981; submitted April 29, 1981; revision received June 14, 1982. Copyright © 1981 by Harold R. Kaufman. Published by the American Institute of Aeronautics and Astronautics with permission.

*Professor and Chairman, Physics Department.
†Assistant Professor, Physics Department.
‡Research Associate, Physics Department.

Hollow Cathodes

Enclosed-Keeper Designs

There is a maximum electron emission that can be obtained with a given combination of hollow-cathode configuration and inert gas flow rate. The limiting condition is a rapid increase in anode voltage when an attempt is made to increase the anode current. No similar limitation has been reported for mercury hollow cathodes. If such a limitation exists with mercury, it probably exists beyond normal operating ranges.

This emission maximum is an important consideration for inert gas thruster design. For example, using tests in a small vacuum chamber as a basis for estimating performance, the reference design utilizing an open keeper described herein would require 0.6 A-equiv of argon to neutralize a 10 A ion beam with a 26% safety margin between normal operation and the emission limit. This means that a factor of about 0.95 would be introduced into the overall thruster efficiency due to just the neutral loss from the neutralizer. If a greater safety margin were used, the reduction in overall efficiency would be greater. A similar calculation for the discharge chamber shows that most of the neutral flow to the discharge chamber would have to be directed through the discharge chamber cathode, or cathodes. Such a cathode flow could easily result in significant propellant density nonuniformities in the discharge chamber for the short length-to-diameter ratios expected in future large thrusters. Means of increasing the maximum emission for a given gas flow are, therefore, of interest for future inert gas thrusters.

Preliminary tests have shown higher electron emissions are possible for the same inert gas flow using an enclosed-keeper design.[5] As a result of these preliminary tests, an extensive study has been conducted to determine the optimum enclosed-keeper configuration. The enclosed-keeper design tested, together with the open-keeper reference design with which it was compared, is shown in Fig. 1. The reference design, shown in Fig. 1a, had a wire keeper with an inside diameter of 4 mm, spaced 1 mm from the cathode tip. The enclosed-keeper design, Fig. 1b, was operated with a range of keeper hole diameters from 2 to 6 mm, in 1-mm increments. The keeper spacing from the tip was varied from 1 to 9 mm, also in 1-mm increments. The hollow-cathode orifice was 0.76 mm for both cathode designs. The anode used in all tests was a perforated cylinder 5 cm in diameter and 7.6 cm long, with the cathode mounted on axis near one end. Past tests have shown that a large anode area, such as this, is necessary when using

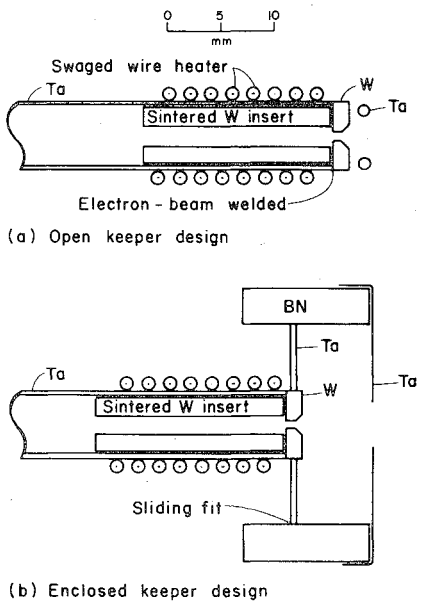

Fig. 1 Hollow-cathode configurations with oxide-impregnated inserts.

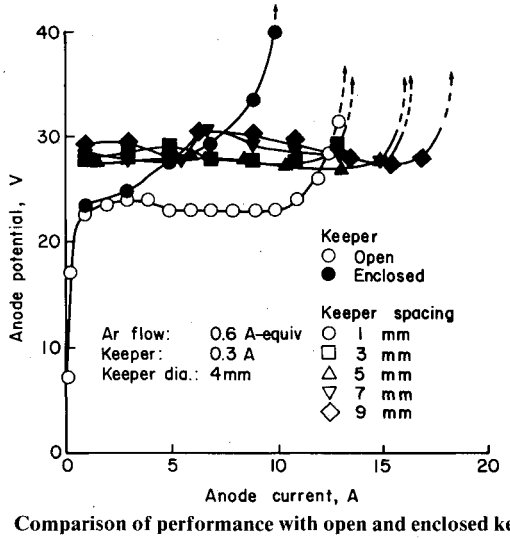

Fig. 2 Comparison of performance with open and enclosed keepers.

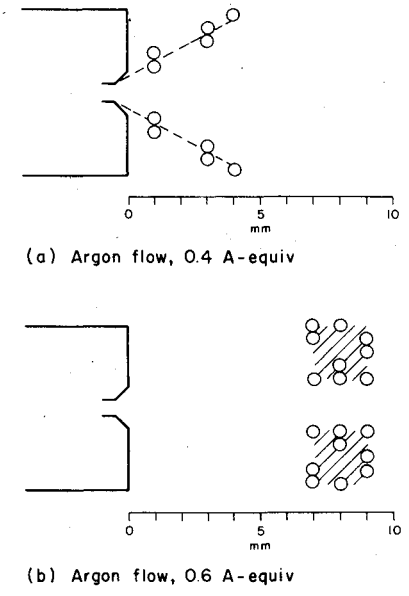

Fig. 3 Optimum enclosed-keeper spacings for a range of keeper opening diameter (optimized for maximum emission at an anode potential of 30 V).

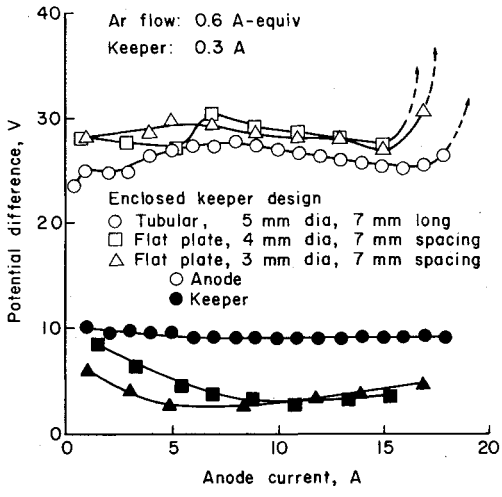

Fig. 4 Comparison of performance with different enclosed-keeper designs.

argon to avoid an increased anode voltage due to the anode sheath. Both open- and enclosed-keeper designs used barium and strontium carbonates for the insert impregnation. The heating prior to operation results in the production of oxides from the carbonates.

Some sample performance curves are shown in Fig. 2 for a 4-mm keeper hole diameter. Note that a sharp rise in anode voltage was encountered for all test configurations, if the emission current was increased to a high enough value. As described in earlier work, operation within this region of sharp voltage rise is associated with a large increase in electrical "noise" and plume luminosity.[5] As indicated in Fig. 2 keeper currents were maintained at 0.3 A. As a result, keeper voltages varied, but were typically in the 5-15 V range.

The optimum enclosed-keeper position is shown in Fig. 3 for each hole diameter investigated. The points shown indicate the position of the aperture in the keeper. (The vertical scale in Fig. 3 is the same as the horizontal scale.) The optimum in this case was defined as the spacing that gave the highest ratio of electron emission to gas flow (A/A-equiv) at an anode potential of 30 V. Where more than one keeper spacing is shown for the same hole diameter, no significant difference was found for the spacings shown.

The mean free path within the keeper enclosure was calculated assuming an enclosure temperature of 400°C and a neutral cross section of 26 Å (Ref. 2). For the 0.4 A-equiv flow rate, the calculated mean free path was, in all cases, larger than the keeper spacings shown in Fig. 4a. This calculated result is consistent with the optimum-keeper locations of Fig. 3a, which roughly define a cone with a 30 deg half-angle. The electron current from a hollow cathode is known to roughly follow the path of the neutral efflux from the orifice. For the 0.4 A-equiv flow of Fig. 3a, the distribution of the neutral efflux appears to be determined close to the orifice, with little effect due to the pressure within the keeper enclosure. The best keeper locations, in this case, resemble those found for open-keeper designs; that is, they do not intrude on the central current carrying region which occupies a large-angle conical volume.[6]

For the 0.6 A-equiv argon flow rate, the calculated mean free paths, in all cases, were smaller than the optimum-keeper spacings of Fig. 3b. This result is consistent with these locations forming much smaller angles relative to the beam axis and the orifice. That is, the higher enclosure pressures at the 0.6 A-equiv flow rate result in a closer approach to

continuum flow, so that the efflux is actually confined to a smaller region due to the pressure within the enclosed keeper. This interpretation is qualitatively consistent with effective enclosed-keeper designs developed for mercury.[6]

At 0.4 A-equiv of argon, the reference open-keeper design had a maximum emission-to-flow ratio of 16 A/A-equiv. For the keeper locations shown in Fig. 4a, the same ratio ranged from 15-28 A/A-equiv, with the highest ratio obtained at the highest spacing.

At 0.6 A-equiv, the reference open-keeper design had a ratio of 21 A/A-equiv. For the keeper locations shown in Fig. 4b, the ratios were 23-33 A/A-equiv, with the lowest ratio obtained using the 2-mm hole and the highest with the 6-mm hole.

The best enclosed-keeper designs thus gave 60-70% increases in emission over the reference open-keeper design at the same gas flow rate. For the orifice size used (0.76 mm), good performance should not be expected much below 0.4 A-equiv of argon. At 0.3 A-equiv, an emission flow ratio of 17 was obtained, but there was an intermediate region of erratic operation that exceeded 30 V. Assuming a design with adequate heat rejection, satisfactory operation should be expected at higher gas flows. At 0.7 A-equiv, the emission flow ratio was 28, or more,§ with the open-keeper reference design. Extrapolation of these trends would indicate that an open-keeper design may be adequate, if emissions and flow rates are high enough. If an enclosed-keeper design is used at higher flow rates, the optimum designs would be expected to be more similar to Fig. 3b than Fig. 3a.

Some experiments were also conducted with various shapes for the keeper enclosure, but without any significant effect on the performance. As an example of these experiments, data for a tubular keeper, 5 mm in diameter and 7 mm long, are shown in Fig. 4. Also shown in Fig. 4 are data for flat-plate keepers (of the type shown in Fig. 1b) with a spacing of 7 mm and diameters of 3 and 4 mm. The flat-plate keeper holes selected were smaller than the tubular hole to approximate the same gas flow impedance. As can be seen, the anode characteristics were quite similar for the two keeper configurations. The keeper voltage for the tubular keeper design was slightly higher, perhaps because the larger 5 mm diameter had a higher impedance connection to the current carrying region near the axis.

Carbon Tip Designs

There appears to be a clear need for large inert gas thrusters in the future, which implies a similar need for large cathodes. The present hollow-cathode design, with a tungsten tip electron beam welded to a tantalum tube, is expensive and difficult to fabricate. Also, the possibility of thermal stress and fatigue problems at the welded joint would be increased with increased cathode size and power.

An alternate approach was considered as a means of avoiding most of the thermal stress problems. In this alternate approach the tip is a separate part, kept in contact with the cathode tube by spring tension. With such a design, relative expansion of the tip and tube can take place without significant stress. Also, with no welding required, the choice of tip material can be made without consideration of welding compatibility. Carbon (graphite) then becomes a good candidate, with excellent high-temperature capability and ease of machining.

The carbon tip design, shown in Fig. 5a, was first tested with an oxide-impregnated insert. Five hours of operation resulted in noticeable material removal from the upstream edge of the orifice, apparently by some flaking process rather than sputter erosion. The glow discharge heating concept, also shown in Fig. 5a was first tested with a conventional

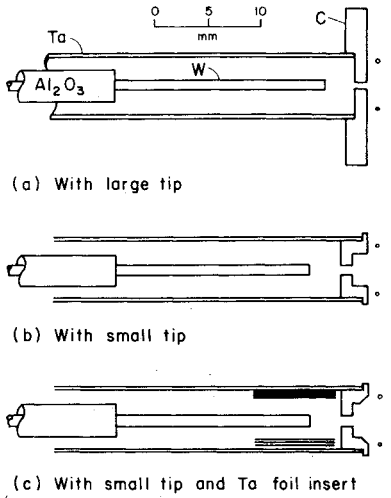

Fig. 5 Carbon tip hollow-cathode configurations investigated, orifice diameter 0.71 mm.

tungsten tip, which reached temperatures in excess of 2000°C during operation. The high temperature encountered without oxide made the combination with a carbon tip appear attractive. The two concepts were combined, as indicated in Fig. 5a, which resulted in a configuration that never achieved coupling to the anode. Although the tantalum tube was heated to a yellow-white heat by the glow discharge within, no significant electron current was ever established to the anode.

To reduce the cooling influence of the large carbon tip, it was reduced in size, as indicated in Fig. 5b. After about 15 s with a 1.2 A heating discharge between the central tungsten electrode and the tantalum tube, with 0.8 A-equiv of argon flowing, the tip reached 1500°C and a discharge was established to the anode. Up to this point the keeper had been at 500 V to assist coupling through the orifice. The heater and keeper power supplies were then both turned off, and the heating was provided by the cathode-anode current. The operating characteristics for this configuration are shown in Fig. 6. The 4-A point represents the lowest anode current for which the cathode was self-heating. The tip temperatures ranged from about 1500°C at 4 A to 1700°C at 15 A. Disassembly after several hours of running revealed some surface texturing, but no significant dimensional changes. Some sputtering damage might be expected for the central starting electrode, inasmuch as a voltage well above the sputtering threshold is required to generate the 1.2 A heating current. The time for this initial heating current is so short, though, that many startups would be required for measurable damage.

A working hypothesis was made at this point. Assuming the required emission temperature¶ is achievable, the potential difference between the cathode and the plasma within it varies to maintain a surface at emitting temperature. For an oxide-coated or impregnated insert, the heating power can be quite low. Without oxide, a much higher power must be supplied to reach emission temperature. Comparing the performance of a conventional hollow cathode that uses oxide[5] with the configuration shown in Fig. 5b, the difference in anode voltage at similar currents indicates an additional 100-120 W of heating power is required in the absence of oxide.

From the above reasoning, an attempt was made to reduce the anode voltage required by providing better thermal isolation between the emitting surface and the outside of the cathode. The emitting surface and the thermal isolation consisted of three layers of tantalum foil inside the tantalum tube. This configuration was first tested without the tip bevel

§The power supply limit was reached before a sharp anode voltage rise was encountered; therefore, the exact maximum ratio is not known.

¶The actual emission within a hollow cathode is believed to be by a combination of thermionic and high-field processes. In this discussion, the concern is primarily with the effects of temperature.

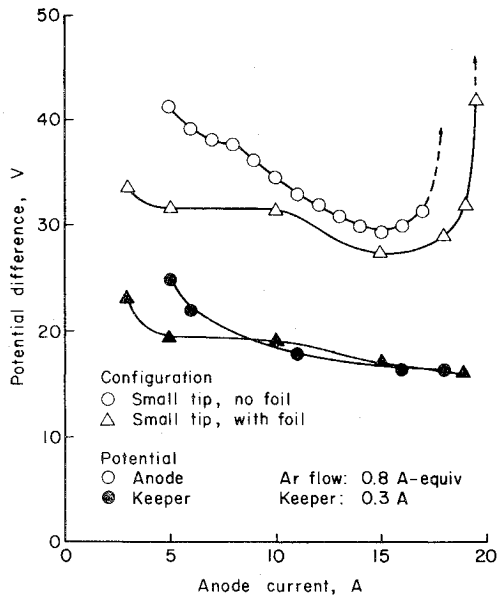

Fig. 6 Hollow-cathode performance with carbon (graphite) tip configurations.

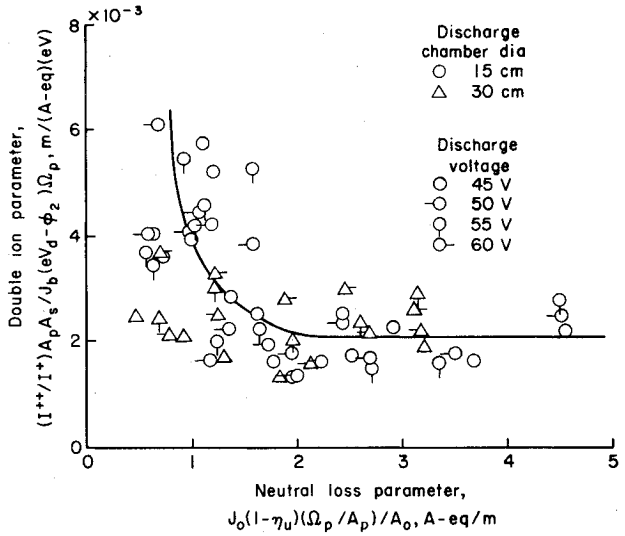

Fig. 7 Double-ion correlation for argon.

also included in Fig. 5c. The major effect of the tip bevel (compare tips for Figs. 5b and 5c) was to increase the maximum anode current by about 2 A. Data for the configuration, as shown in Fig. 5c, are also shown in Fig. 6. Comparing the data for the two configurations in Fig. 6, the addition of the tantalum foil reduced the heating power requirements by 30-50 W.

An even more impressive result of the tantalum foil addition was the ease of starting. Starting at room temperature with a 1.1 A-equiv argon flow and 65 V on the anode (no keeper), the 1.2 A internal discharge would heat the cathode to emission temperature and permit coupling to the anode within 5 s. The heater power could then be turned off, the flow reduced to 0.7 A-equiv, and normal operation maintained over a 3-20 A emission range. The tip temperature for this configuration ranged from a little over 1200°C at 3 A to over 1800°C at 19 A. Disassembly after several hours of operation revealed no measurable erosion.

The results presented for carbon tip hollow cathodes, without oxide-enhanced emissive surfaces, are believed to be significant. These results suggest that the present electron beam-welded construction can be replaced with a more economical assembled construction. Also, it is possible that oxides, with their attendant problems of conditioning, poisoning, and depletion, might be eliminated. Some additional heating power (and hence coupling voltage) will probably be required in the absence of oxide, but with proper thermal design, this increase should be small. Note that the glow discharge heater is inherently simpler than the swaged wire heater that it replaces, indicating the possibility of increased heater reliability.

Doubly Ionized Propellant

The erosion within the discharge chamber of a thruster is due mostly to doubly charged ions. This erosion has become more serious as thrusters become larger, and two-step double ionization from primary electrons has become the dominant process at normal operating conditions.** With even larger thrusters planned for the future, the prediction and control of doubly ionized propellants have become an important research area.

**A one-step process is involved when a neutral becomes a doubly charged ion with a single electron collision. A two-step process requires two electron collisions for a doubly charged ion to be generated from a neutral, with a singly charged ion the usual intermediate step.

A theory for the production of doubly charged ions has existed for some time.[7,8] but the utility of this theory has been limited by the prior need for detailed plasma probe data. A more recent approach assumes that the two-step process from primary electrons is the dominant one for generating doubly charged ions.[9] With this assumption, parameters were derived for use in the correlation of experimental double ion data, without any requirement for detailed plasma properties. The correlation of experimental data obtained was also in qualitative agreement with a straight theoretical derivation using the same two-step assumption.

The experimental data used in the correlation described above were obtained with a 15-cm multipole thruster. With much larger thrusters planned for the future, it is of interest how well the data from larger thrusters would agree with the correlation. Double ion data were therefore obtained from a 30-cm multipole thruster. These 30-cm data are plotted in Fig. 7, together with the previously obtained 15-cm data. The curve in Fig. 7 is the one used previously to fit just the 15-cm data. In the neutral loss parameter, J_0 is the total neutral flow rate to the discharge chamber in A-equiv, η_u is the fraction of this total flow that is ionized when it leaves the discharge chamber, Ω_p and A_p are the volume and outside area of the primary electron region in m^3 and m^2, and A_0 is the effective sharp-edged orifice area for the escape of neutrals through the ion optics. The 15- and 30-cm discharge chambers were cylindrical multipole designs of moderate field strength ($\int B dx = 70$-80 G-cm). The primary electron region in these designs was assumed to be cylindrical in shape, just fitting inside the screen grid, pole pieces, and anodes. The effective area A_0 includes both the open area of the optics and the Clausing factor for free molecular flow through the cylindrical sections. In the double-ion parameter, in addition to some of the above quantities, I^{++}/I^{+} is the ratio of doubly to single ionized ion currents, A_s is the open screen area for extracting ions in m^2, J_b is the ion beam current in A, eV_d is the primary electron energy in eV (electronic charge times discharge voltage), and ϕ_2 is the second ionization potential in eV.

The 30-cm data in Fig. 7 show substantial agreement with the previously obtained 15-cm data. Data were also obtained with the 30-cm discharge chamber at a discharge voltage of 70 V, although these data are not included in Fig. 7. Compared to the data obtained at lower discharge voltages, the 70-V data had much higher double-ion ratios, presumably because of the greater importance of the one-step production of double ions.

To check the effect of the one-step process on the 30-cm data, the derivation of the double-ion parameter was

repeated, except that both the one- and two-step production of doubly charged ions from primary electrons were included.†† This modified double-ion parameter resulted in a much improved correlation of data, especially the data obtained at high discharge voltages. Unfortunately, the modified parameter is also much more complicated, in that it must include cross sections for both one- and two-step processes at primary electron energy. Also, most thruster applications are limited to small double-ion fractions, where the one-step process is, indeed, small.

For thruster applications, then, the correlation indicated by the 15- and 30-cm data is recommended for design-stage predictions. The agreement between 15- and 30-cm data (at moderate discharge voltages) indicates that extrapolation to even larger thruster sizes may be reasonable. A careful comparison of the more complicated correlation described above with the correlation indicated in Fig.7 indicates that the average contribution of one-step double ionization may be as much as 40% of the total double ionization measured. The double-ion correlation of Fig. 7 thus represents a dominant two-step process, but still with a significant contribution from the one-step process.

Ion Reflection Experiment

Electric propulsion applications would, in general, benefit from lower discharge losses. This is particularly true for lower specific impulses, where the effect of discharge loss on overall efficiency is greater. One of the approaches to reducing discharge losses that has been studied in the past is ion reflection at the boundaries of the discharge chamber.

To the first approximation, ions produced in a discharge chamber tend to propagate equally in all directions. The discharge losses per extracted ion are, therefore, roughly proportional to the total area around the production region divided by the extraction area. The production region is, of course, approximated as the primary electron region, where primary electrons cannot be intercepted by the anode without first undergoing a collision. The approach of interest here is the possible reflection of ions at a nonextraction boundary, thus reducing the effective loss area for ions.

The first clear description of this ion reflection concept in the electric propulsion field was by Moore[10] and Ramsey.[11] It was referred to as magnetoelectrostatic containment, or MESC. In MESC the anodes were biased positive of the discharge plasma, so that ions approaching the anodes would be reflected, saving them for extraction into the ion beam. Using this approach, Ramsey reported Hg discharge losses of 155-160 eV/ion at 90% utilization. This loss was approximately two-thirds of what would be expected from the extraction area and the area surrounding the production region. It, therefore, appears clear that some degree of reflection was actually taking place.

The experiment to be described next was not successful, in the sense that ion reflection was not achieved. It should be of interest, however, for any program directed at reducing discharge losses.

The anodes of a rectangular beam multipole ion source[12] were biased, as indicated in Fig. 8. The relative bias between the two sets of anodes was small compared to the total discharge voltage, so both sets were still positive relative to the electron-emitting cathode. An anode was not installed where the cathode supports are indicated. Otherwise, all the anodes opposite the ion optics were biased positive relative to the other anodes. The discharge power was assumed to be the total of the powers through the two sets of anodes.

It was hoped that the positively biased anodes would become positive relative to the discharge plasma. Such a bias

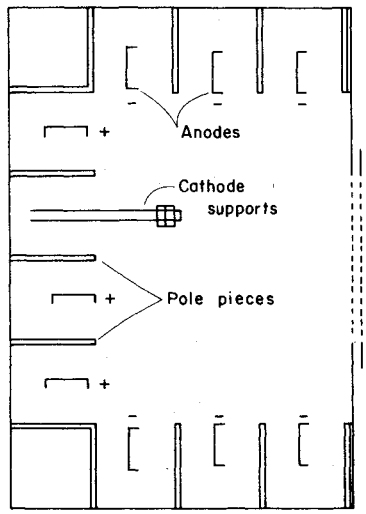

Fig. 8 Anode bias configuration used in rectangular-beam thruster.

was, indeed, verified in separate tests with Langmuir probes. For a 10-V positive bias on the anodes indicated in Fig. 8, for example, the plasma potential increased only 1 V. With the plasma initially being several volts positive of the anodes, a 10-V bias was sufficient to make the positive anodes more positive than the plasma.

It was also hoped that the bias would, at some point, result in ion reflection and reduced discharge losses. No such reduction took place. At small bias voltage, the effect on discharge loss was negligible. As the bias voltage was increased, the discharge loss increased at an increasing rate.

As indicated earlier, this test was not successful in that it did not achieve the hoped for reduction in discharge losses. Inasmuch as the anodes could be biased positive of the discharge plasma, the lack of ion reflection still remains to be explained. At this point, the best explanations appear to involve magnetic field strength and transient behavior.

The diffusion of electrons across the magnetic field to the anodes has been shown to be in the "anomalous" or "turbulent" diffusion regime.[9] That is, the electron diffusion across the magnetic field is not a steady-state process. Instead, it is accompanied by fluctuations in density and potential. Thus, despite a time-averaged potential that would tend to reflect ions, the fluctuations could still permit ions to reach the vicinity of the anodes.

The magnetic field integral ($\int B \times dX$) between the bulk of the discharge chamber and an anode was, for the rectangular beam ion source, just sufficient to deflect primary electrons back into the discharge chamber. For the discharge chamber used by Ramsey, the magnetic integral was several times higher. So high, in fact, that a separate "plasma anode," unprotected by magnetic field, was required for the completion of the discharge circuit. This difference in magnetic field integral may have been sufficient to permit some ion reflection despite the fluctuations expected in the diffusion process. At this point, however, the information is not sufficient to draw a clear-cut conclusion.

Single-Grid Ion Optics

Electric propulsion offers substantial payload advantages over chemical rockets for geocentric orbit-raising missions. Trip time, however, is often a serious concern for such missions. To minimize the increased trip time normally associated with electric propulsion orbit-raising missions, relatively low specific impulses are of interest.

With both two-[13] and three-grid[14] ion optics, the space charge between the grids serves to limit the possible ion-beam current density at low specific impulses. Decreasing the spacing between grids will increase the ion current density, but

††Doubly charged ions can also be produced by the background Maxwellian electrons. The Maxwellian electron temperatures, however, tends to decrease with increasing thruster size, so this process becomes relatively unimportant for large thrusters.

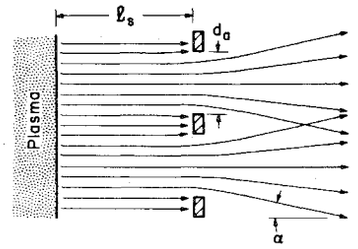

(a) Large relative sheath thickness

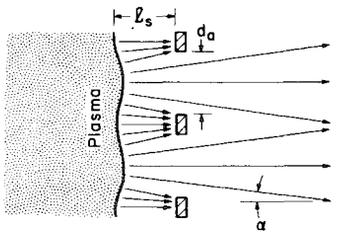

(b) Small relative sheath thickness

Fig. 9 Single-grid operation at different relative sheath thicknesses (ℓ_s/d_a).

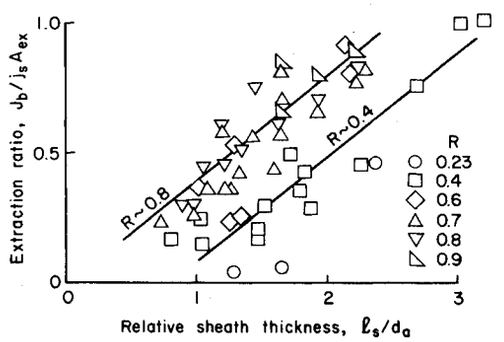

Fig. 10 Single-grid performance for a range of net-to-total voltage range, R.

there are practical limits involved in this reduction of grid spacing.[15]

Single-grid optics have been used to generate very low-energy ion beams,[16,17] but have not previously been proposed for electrostatic thrusters. As discharge chambers become more efficient, the permissible minimum specific impulse from an efficiency viewpoint drops. If the ion energy is permitted to be low enough, it will approach the sputtering threshold and adequate lifetime will be assured. For example, a 30-eV argon ion (near the sputtering threshold) still has a velocity corresponding to about 1200 s.

The major performance considerations for single-grid ion optics, besides durability, are the fraction of ions transmitted and the divergence characteristics of the transmitted ion beam. If, as indicated in Fig. 9a, the ion sheath, ℓ_s, is large compared to the accelerator hole diameter, d_a, the accelerated ions will "see" a nearly uniform potential at the accelerator grid. The fraction of ions escaping into the ion beam will then approximate the open-area fraction of the accelerator. If, on the other hand, as indicated in Fig. 9b, the sheath thickness approaches the accelerator hole diameter, a larger fraction of the ions will be directed toward the accelerator grid.

The sheath thickness is, of course, determined by the ion current density arriving at the sheath, the potential difference between the plasma and the accelerator grid, and the charge-to-mass ratio of the ion being accelerated. For the sheath thicknesses presented herein, calculated values from Child's law were used; that is, a simple one-dimensional planar distribution of potential was assumed, with no correction for the apertures in the accelerator grid. The plasma potential was

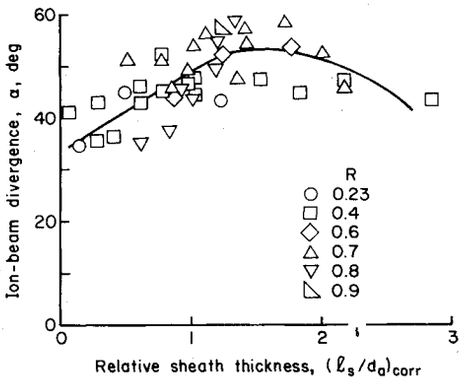

Fig. 11 Ion-beam divergence as a function of ℓ_s/d_a, with the latter corrected to a net-to-total voltage ratio of 0.8.

assumed equal to anode potential, while the minimum sheath potential equaled that of the accelerator grid. The ion current density was obtained from the beam current, impingement current, and total beam area. The central portion of a large multipole thruster was used to assure uniformity over the ~1 cm beam diameter used. The open area fraction of the accelerator used was 43%. A much higher open-area fraction would be required for an actual propulsion application. The test voltages were high (up to 500 V) for single-grid operation. This was because the available grid had large 1.6-mm apertures, and high voltages were required to obtain comparable sheath thicknesses at reasonable ion-current densities.

The extraction ratio is the ion current actually extracted divided by the product of ion-current density at the sheath and the accelerator open area, J_b/j_sA_{ex}. This extraction ratio is presented in Fig. 10 as a function of relative sheath thickness, ℓ_s/d_a. It is clear from the data distribution that, for the same value of ℓ_s/d_a, the extraction ratio increases monotonically with R, the net-to-total voltage ratio.

The variation in extraction with R might be expected from the aperture effect at the accelerator grid. As R is decreased, the potential distribution within the apertures will change in order to deflect more ions into the accelerator grid. This increased impingement due to a decreased R, can, of course, be offset by an increase in sheath thickness, so that the ions acquire a greater fraction of their total energy before reaching the vicinity of the accelerator aperture. Inversely, one might expect to correct the performance to a higher value of R by subtracting some fraction of the sheath thickness. Experimentally, this correction of ℓ_s/d_a due to R was found to be about

$$\Delta\ell_s/d_a \sim -2/(0.8-R) \tag{1}$$

with 0.8 used as the reference value of R.

The correction of Eq. (1) can be carried a step further and used to obtain the extraction ratio, J_b/j_sA_{ex}, as a function of relative sheath thickness and R.

$$J_b/j_sA_{ex} \sim 0.4(\ell_s/d_a) - 0.8(0.8-R) \tag{2}$$

If the extraction ratio J_b/j_sA_{ex} from this equation exceeds 1.0, a value of 1.0 should be used instead. This is because there is no physical reason to expect ions to be deflected away from the accelerator grid for R values less than 1.0. And R values less than 1.0 are required to prevent electron backstreaming. Within this limit of extraction ratio being ≤ 1, Eq. (2) correlated the experimental results to within ± 0.15.

Several means of correlating the ion-beam divergence angle were tried, with Fig. 11 showing the clearest correlation. The angle α shown in Fig. 11 is the half-angle that encloses 95% of the total ion beam. Within the half-angles shown in Fig. 11, the beam profiles were fairly smooth and symmetrical. The current density was typically half the peak value at angles half as large as shown in Fig. 11.

As shown by the experimental data, high extraction ratios can be achieved at sheath thicknesses several times the accelerator hole diameter. If a high open-area fraction is used for the accelerator grid, the fraction of ions extracted should also be high. The beam divergence can be quite large, as indicated by Fig. 11. The beam divergence can be expected to decrease if ℓ_s/d_a is increased beyond the range shown in Fig. 11. The results shown are limited in that only one accelerator-grid configuration was used. These results should, however, still be useful for performance estimates.

Concluding Remarks

Compared to previous tests with an open keeper, an enclosed-keeper hollow cathode gave 60-70% higher electron emissions. At an argon flow of 0.4-0.6 A-equiv, the enclosed-keeper design gave emission-to-flow ratios of 28-33 A/A-equiv. In comparison, the open-keeper design only reached 16-23 A/A-equiv.

A hollow cathode with a carbon tip and a glow-discharge heater was also operated. Unlike the conventional hollow-cathode design, no emissive oxide was used. Comparison with the performance of a conventional hollow cathode indicated that an additional anode-cathode voltage was required, which provided the extra heating power for operation without oxide. The carbon tip design appears promising for larger hollow cathodes, where use of the conventional design could result in serious thermal stresses at the tip weld.

Double-ion data from a 30-cm thruster operated at moderate voltages indicated agreement with a double-ion correlation obtained previously with data from a 15-cm thruster. This agreement indicates that extrapolation to even larger thruster sizes may be reasonable. Operation at moderate discharge voltages is important if the assumed two-step double-ionization process is to dominate. This assumption, however, should be easily met with designs intended to have long lifetimes.

An ion reflection experiment was conducted with some of the anodes biased relative to the rest. It was hoped that ion reflection would take place when the positively biased anodes became more positive than the discharge plasma, resulting in reduced discharge losses. Although some anodes became more positive than the discharge plasma, no reduction in discharge losses was observed. The most likely explanations for the absence of ion reflection appear to involve the magnetic field strength used and the fluctuations known to exist near the anodes.

A single-grid ion-optics configuration was evaluated for possible use, for electrostatic thrusters, at low specific impulses. The transmitted ion current increased with the ratio of sheath thickness to accelerator hole diameter up to a ratio of 2-3. At this ratio the transmitted ion current corresponded to about the projected open area of the accelerator. The half-angle of beam divergence was quite large, ranging from about 30-60 deg (for 95% of the beam within this angle). A reduction in this half-angle would be expected for larger sheath thicknesses—more than 2-3 times the accelerator hole diameter. The maximum useful specific impulse for single-grid optics is limited due to the sputtering from direct-ion impingement. Within this limit, though, the single-grid approach offers a means of avoiding the usual span-to-gap limits of multiple-grid ion optics.

Acknowledgment

This work was performed under NASA Grant NSG 3011.

References

[1] Kaufman, H.R., "Experimental Investigations of Argon and Xenon Ion Sources," NASA CR-134845, June 1975.

[2] Kaufman, H.R., "Inert Gas Thrusters," NASA CR-135100, July 1976.

[3] Kaufman, H.R., "Inert Gas Thrusters," NASA CR-135226, July 1977.

[4] Kaufman, H.R., "Inert Gas Thrusters," NASA CR-159527, Nov. 1978.

[5] Kaufman, H.R. and Robinson, R.S., "Inert Gas Thrusters," NASA CR-159813, Nov. 1979.

[6] Kaufman, H.R., "Technology of Electron-Bombardment Ion Thrusters," in *Advances in Electronics and Electron Physics*, Vol. 36, Academic Press, New York, 1974, pp. 265-373.

[7] Peters, R.R., "Double Ion Production in Mercury Thrusters," NASA CR-135019, April 1976.

[8] Wilbur, P.J., "Argon-Xenon Discharge Chamber Model for the Production of Doubly Charged Ions," pp. 46-64 of Ref. 3, NASA CR135226.

[9] Kaufman, H.R. and Robinson, R.S., "Plasma Processes in Inert Gas Thrusters," *Journal of Spacecraft and Rockets*, Vol. 18, Sept.-Oct. 1981, pp. 470-476.

[10] Moore, R.D., "Magneto-Electrostatically Contained Plasma Ion Thruster," AIAA Paper 69-260, March 1969.

[11] Ramsey, W.D., "12-cm Magneto-Electrostatic Containment Mercury Ion Thruster Development," *Journal of Spacecraft and Rockets*, Vol. 9, May 1972, pp. 318-321.

[12] Robinson, R.S., Kaufman, H.R., and Haynes, C.M., "A 5×40 cm Rectangular-Beam Multipole Ion Source," AIAA Paper 81-0667, April 1981.

[13] Aston, G., Kaufman, H.R., and Wilbur, P.J., "Ion Beam Divergence Characteristics of Two-Grid Accelerator Systems," *AIAA Journal*, Vol. 16, May 1978, pp. 516-524.

[14] Aston, G. and Kaufman, H.R., "Ion Beam Divergence Characteristics of Three-Grid Accelerator Systems," *AIAA Journal*, Vol. 17, Jan. 1979, pp. 64-70.

[15] Kaufman, H.R. and Robinson, R.S., "Ion Source Design for Industrial Applications," AIAA Paper 81-0668, April 1981.

[16] LeVaguerése, P. and Pigache, "Étude d'une source d'ions de basse énergie et á forte densité de courant," *Revue de Physique Appliquée*, Vol. 6, Sept. 1971, pp. 325-327.

[17] Harper, J.M.E., Cuomo, J.J., Leary, P.A., Summa, G.M., Kaufman, H.R., and Bresnock, F.J., "Low Energy Ion Beam Etching," *Proceedings of Symposium on Electron and Ion Beam Science and Technology*, Vol. 80-6, Electrochemical Society, Pennington, N.J., 1980, pp. 518-530.